

## **Application of Electrochemical Impedance Spectroscopy in the Evaluation of Corrosion and Cathodic Protection in Reinforced Concrete**

D.A.Koleva<sup>a</sup>, K.van Breugel<sup>a</sup>, J.H.W.de Wit<sup>b</sup>, A.L.A.Fraaij<sup>a</sup>, N.Boshkov<sup>c</sup>

<sup>a</sup>Delft University of Technology, Department Civil Engineering and Geosciences,  
Section Material Science, 2628 CN Delft, The Netherlands

<sup>b</sup>Delft University of Technology, Faculty of Materials Science and Engineering,  
Corrosion technology & Electrochemistry Department, Mekelweg 2, 2628 CD Delft,  
The Netherlands

<sup>c</sup>Bulgarian Academy of Sciences, Institute of Physical Chemistry, Acad.G.Bonchev bl.11,  
Sofia, Bulgaria

The electrochemical behavior of steel reinforcement in conditions of corrosion and cathodic protection (CP) was studied, using electrochemical impedance spectroscopy (EIS) and compared to reference (non-corroding) conditions. Polarization resistance (PR) method and potentiodynamic polarization (PDP) were employed as well, in addition to AC 2 pin electrical resistance monitoring, thus deriving a comparison of the involved parameters. It was found out that EIS is readily applicable for evaluating electrochemical behavior of the steel surface not only for corroding or passive state, but also in conditions of CP, although the interpretation of derived parameters is not straightforward and is related to the properties of the product layers, formed on the steel surface in the different conditions. The evaluation of the electrochemical behavior of the steel surface, should take into account the crystallinity, morphology and composition of the surface layers, which were investigated by scanning electron microscopy (SEM) and energy dispersive X-ray analysis (EDAX).

### **Introduction**

In non-damaged reinforced concrete, steel remains passive due to the high alkalinity of the concrete pore solution (pH 12.5 to 13.5). If damages of the concrete cover and the concrete bulk matrix occur, depending on the aggressiveness of the environment, corrosion of the steel reinforcement will be initiated. The initiation and further evolution of the corrosion process will depend on the concrete pore network permeability and connectivity on one hand and the rate of penetration, amounts and concentration of aggressive substances in the environment (CO<sub>2</sub>, chlorides, sulphates) on the other. In the presence of chlorides, localized corrosion takes place as consequence of passive layer break down. The rate of the process depends to a significant extent on the initial surface state of the steel surface, the chloride concentration, the chloride binding capacity of the bulk concrete matrix etc. The chloride-induced corrosion process on steel reinforcement has been largely studied in concrete and in simulated pore solutions as well (1-21). Along with the localized corrosion on the steel surface, physico-chemical and structural transformations are taking place on the steel/cement paste interface. Further, the morphological alterations and certain distribution of product layers are influencing the mechanical properties of the reinforced concrete system as a whole.

Impressed current cathodic protection (ICCP) is one of the protection techniques, applied to such systems. Along with minimizing the corrosion process and preventing further corrosion on the steel surface, CP is known to have secondary positive effects of chloride withdrawn from the steel/cement paste interface. Side effects however are known in these applications as well e.g. bond-strength degradation, alkali ion accumulation and possible concrete degradation due to alkali-silica reaction etc.(22,23)

The present study aimed at:

- Investigation the applicability of electrochemical techniques (EIS, PDP, PR) in monitoring the steel parameters in conditions of corrosion and cathodic protection in reinforced concrete.

- Further, based on obtained results, to evaluate if the introduced cost-effective ICCP, denoted as pulse CP, is as effective as the conventional CP.

- Additionally, the correlation was expected to supply information for the properties and performance of product layers, formed on the steel surface in every technical condition and to provide evidences for the fundamental mechanisms of CP efficiency, which is normally evaluated according empirical criteria only.

### Experimental materials and methods

The materials used in the present study were reinforced concrete cylinders, cast from OPC CEM I 32.5, w/c ratio 0.6, with dimensions: H=25cm, D=12 cm, embedded construction steel (d=12mm). The experimental set-up (generally used by the authors (24) is presented on Fig.1.

Aiming at initiation of corrosion before applying CP, the specimens were maintained in a salt spray chamber (SSC -5% NaCl, 25 to 35°C) for 460 days after curing in fog room conditions (98% RH and 20°C) for 28 days. Additionally, the specimens were immersed 1/3<sup>rd</sup> in 5% NaCl for the whole period of SSC conditioning (except for the non-corroding cells, maintained in the same RH and temperature conditions, but immersed in water).

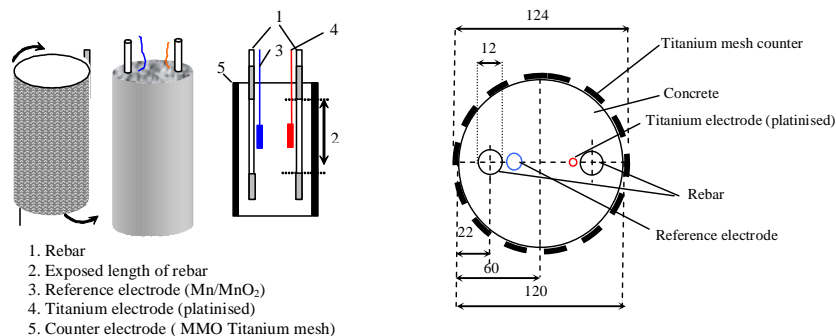


Fig. 1 Experimental set-up

Four main groups of specimens were investigated: a freely corroding group (further in the text represented by specimen 3), a non-corroding group (represented by specimen R), group with applied conventional CP (represented by specimen 6) and a group with applied pulse CP (specimen 7).

Cathodic protection was employed in the two regimes (conventional and pulse), using DC current in the range of 5 to 20 mA/m<sup>2</sup> steel surface, duty cycle for the pulse regime was 12.5% to 50 % at 1kHz frequency. The protection was applied after corrosion was initiated, at certain intervals for different cell-couples. The presented results are for

specimens, on which CP was applied at 120 days of age i.e. in the time of applying protection, corrosion was already in an advanced stage. The collected data in this study are for 270 days of age, when conditioning of the specimens was interrupted for investigation.

The electrochemical methods involved were electrochemical impedance spectroscopy (EIS), potentio-dynamic polarization (PDP) and polarization resistance method (PR). The measurements were performed at open circuit potential (OCP) for all cells (after 24 h depolarization of the reinforcement for the protected specimens i.e. protection current was interrupted before and in the time of the measurement) and in immersed condition (mentioned above), assuring electrical conductivity of the medium. For LPR an external polarization in the range of  $\pm 20$  mV vs OCP was used at scan rate 0.16 mV/s, PDP was performed in the range of -0.15 V to +1.2 V vs OCP. The EIS measurements were carried out in the frequency range of 50 kHz to 10 mHz by superimposing an AC voltage of 10 mV. The used equipment was EcoChemie Autolab - Potentiostat PGSTAT30, combined with FRA2 module, using GPES and FRA interface.

Relevant to the morphological aspects of the product layers, formed on the steel surface in every technical condition, section images of the specimens were obtained by scanning electronic microscopy (SEM), using environmental SEM (ESEM Philips XL30) in backscattered electrons mode (BSE). The chemical composition and distribution of products, associated with corrosion and cathodic protection, were determined using energy dispersive X-ray analysis (EDXA).

## Results and discussion

### 1. Electrochemical methods

Electrochemical impedance spectroscopy (EIS) has emerged as an effective method to distinguish fundamental processes occurring during corrosion and is used as a useful technique for obtaining detailed knowledge of the steel/concrete system. It provides information on a number of parameters, such as the presence of surface films, bulk concrete characteristics, interfacial corrosion or transformation of corrosion product layers, mass transfer phenomena.

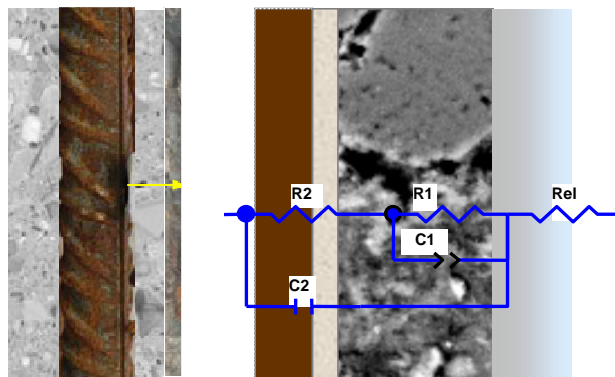


Fig.2 The reinforced concrete system (left), presented by equivalent electrical circuit (right).

The aim of this study was to compare the electrochemical behaviour of the steel surface in conditions of corrosion and CP, using EIS and supportive PDP and PR measurements. The derived parameter was mainly polarization resistance ( $R_p$ ), which can be associated with the corrosion process (the anodic oxidation of steel) as well as other electrochemical processes involving corrosion products.

The equivalent circuit used in the present study comprises two time constants in series with the electrolyte resistance – Fig.2.

The elements of the equivalent circuit present the following physical meaning:  $R_{el}$  is the electrolyte resistance (including contribution of the concrete cover resistance). The first time constant ( $R_1$  and  $C(CPE)_1$ ) is attributed to the properties of the concrete matrix in terms of pore network and properties of product layers on the steel surface. The second time constant ( $R_2$  and  $C(CPE)_2$ ) deals with the electrochemical reaction (or oxi-redox reactions) on the steel surface.

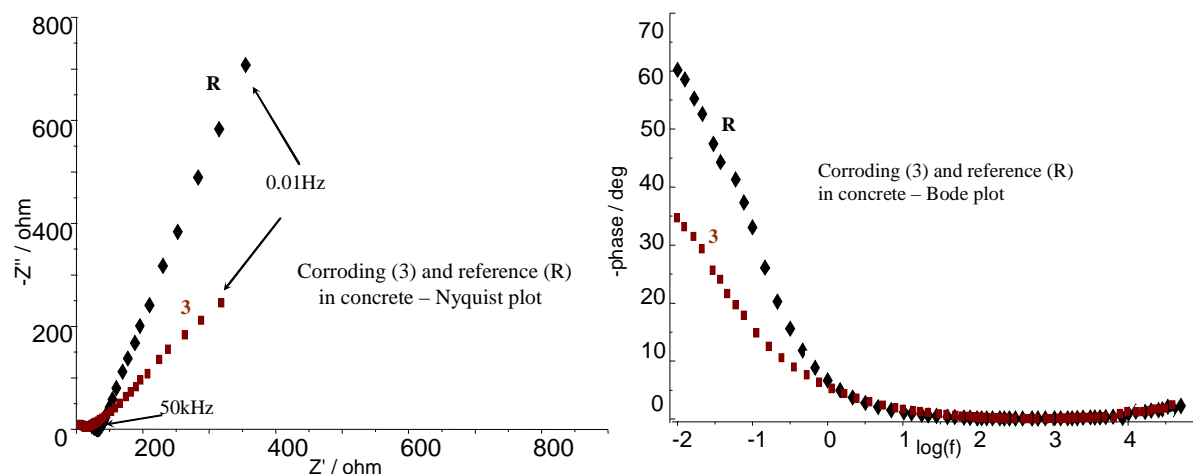


Fig.3 EIS response in Nyquist (left) and Bode (right) format for non-corroding (R) and corroding specimen (3) in concrete at 270 days of age.

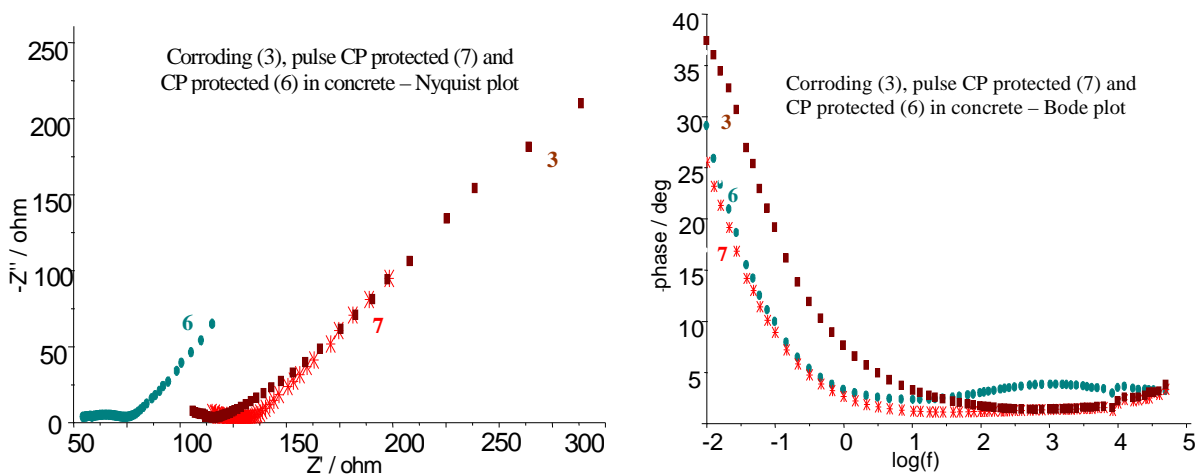


Fig.4 EIS response in Nyquist (left) and Bode (right) format for corroding specimen (3) and protected specimens (6 – CP and 7 – pulse CP) in concrete at 270 days of age

The replacement of pure capacitance ( $C$ ) with constant phase element ( $CPE$ ) in some fitting procedures is widely used and accepted for systems as in this study (2,5,16,25),

being denoted to inhomogeneities at different levels, relevant to the steel surface and to the bulk concrete matrix as well. The CPE is defined as empirical description of the impedance response as:  $Z = (j.\omega)^{-n}/Y_0$ , further quantified by the parameters CPE constant  $Y_0$  and CPE factor  $n$  (26).

For deriving  $R_p$  in EIS applications in reinforced concrete, the system response at lowest frequency is generally considered for calculations as reported in (15,16,27-30) and used in the present study as well. Fig.3 presents the impedance response for non-corroding and corroding specimens (measurements in concrete) in Nyquist and Bode format. Fig.4 depicts an overlay of the impedance response for the corroding specimen and the two types of protected specimens (conventional CP (6) and pulse CP (7)). Summarized data for the best fit parameters are given in Table 1.

Table 1. Best fit parameters from experimental EIS results in concrete

concrete	$R_{el}$ Ohm	$R_1$ Ohm	$C_1$ mF	$C_2$ mF/cm2	$R_2(R_p)$ kOhm.cm2
CP(6)	72.35	19.30	18.80	1.42	17.50
Pulse CP(7)	132.00	42.60	26.80	1.87	27.04
Corroding (3)	108.30	87.80	8.75	0.32	56.70
Reference (R)	156.30	545.00	9.74	0.08	424.00

The high frequency arcs for all specimens correspond to the electrolyte resistance including the contribution of concrete cover (bulk) resistance. The derived  $R_{el}$  values (Table 1) are consistent with derived concrete resistance from AC 2 pin method (generally accepted method for measuring concrete electrical resistance) – Fig.5.

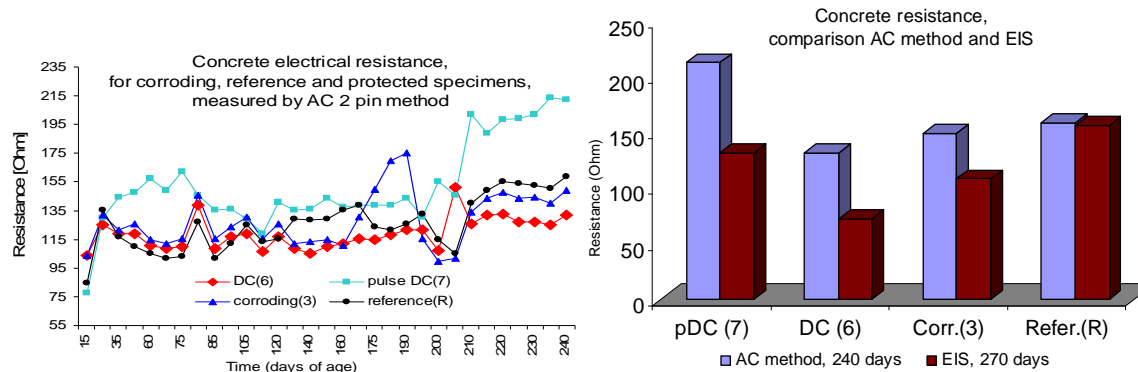


Fig.5 Concrete electrical resistance, derived from AC 2 pin method (left) and comparison of resistance values, derived from AC 2 pin and EIS measurements (right)

As expected, due to volume expansion of corrosion products and micro-cracks initiation, lower resistance was recorded for the corroding specimen (108.3 Ohm), compared to reference specimen (156.3 Ohm). Generally, in terms of cement chemistry and development of microstructural properties with aging, concrete hydration is the main factor influencing the concrete resistance. At the age of 270 days however, more significantly contributing factors are the environmental and technical conditions. As seen from Table 1, the lowest resistance is recorded for the specimen under conventional CP (about 73 ohm), denoted to the influence of current flow on the bulk matrix and bond-strength degradation. In this respect, the pulse CP has beneficial effects, as concrete

resistivity in specimen 7 (pulse CP) is close to non-corroding conditions (specimen R). More detailed information on microstructural properties, related to mechanical performance is already reported by the authors in (31).

The slight deviation between values obtained by the two methods (Fig.5 right) is attributed first to the 30 days difference in age (AC 2 pin method was performed up to 240 days of age) and second – due to the AC 2 pin measurement itself. The measuring device recorded resistance values automatically 4 times per day, hence the CP current flow through the protected cells might have influenced the recorded resistance values, as the deviation for corroding (3) and reference (R) specimens is lower. On the other hand, the resistance of specimen R, being non-corroding, is not expected to give large deviations for 30 days difference at this age, as it is supposed to happen with the other cells as consequence from internal micro-cracking (due to volume expansion of corrosion products or alterations in mechanical properties due to current flow). Hence, it is assumed that microstructural changes due to corrosion and current flow, along with the difference in age, are the reason for the slight deviation in recorded values by EIS and AC methods. Main outcome from the correlation of the two methods is that EIS is able to provide reliable data for electrical properties of concrete bulk matrix as well, along with describing the electrochemical behavior of the steel surface, which will be discussed in what follows.

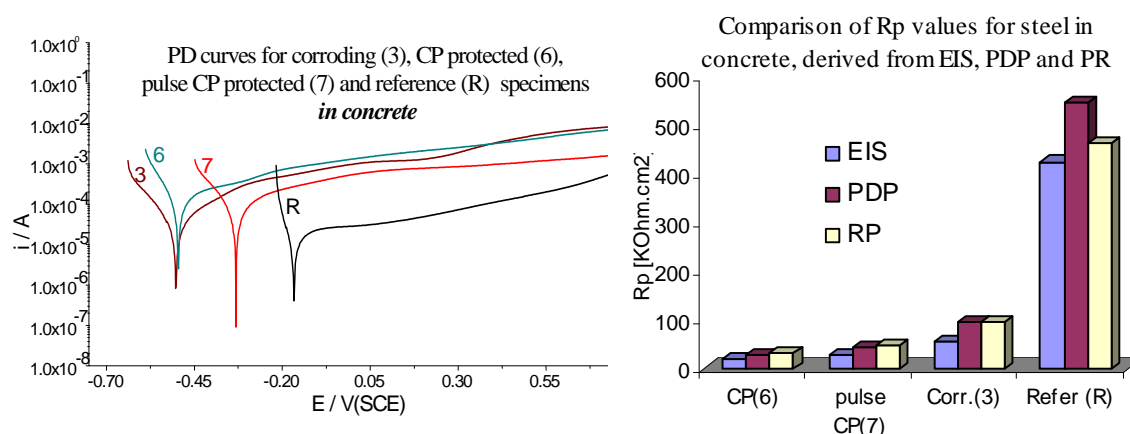


Fig.6 Potentio-dynamic curves for all investigated specimen-groups in concrete (left) and comparison of  $R_p$  values, derived by all electrochemical methods (right)

As mentioned, the response at the lowest frequency was used for deriving  $R_p$  from the EIS measurements in concrete. Fig.3 shows the significant difference of the impedance response for corroding (3) and non-corroding (R) specimens in the high frequency domain, attributed to accelerated corrosion state in the former and passive condition in the latter case. The derived  $R_p$  for corroding specimen is at least one order of magnitude lower compared to non-corroding specimen (Table 1). The corresponding interfacial capacitance ( $C_{dl}$ ) for corroding specimen is higher ( $0.32 \text{ mF/cm}^2$ ), compared to non-corroding specimen ( $0.08 \text{ mF/cm}^2$ ), attributed to spreading the corrosion damage on a large surface area.

Comparing the impedance response for protected specimens and corroding specimen (Fig.4), it is obvious that the magnitude of impedance (Fig.4 left) and phase angle (Fig.4 right) are higher for the corroding specimen. Although it is expected that the protected specimens will exhibit higher impedance and higher  $R_p$  values respectively, apparently this is not the case. The derived  $R_p$  from for corroding specimen is higher (about 57

kOhm.cm<sup>2</sup>) compared to protected specimens (in the range of 18 – 27 kOhm.cm<sup>2</sup>) (Table 1). The observation is consistent with PDP and PR measurements, giving  $R_p$  values in the same range and same trend of change (Fig. 6 right). Generally two mechanisms are most likely responsible for the lower  $R_p$  values in protected conditions. First, maintaining the steel in protected specimens cathodic during the time of the experiment (270 days), with interruptions of the protection current only in the time of depolarization and electrochemical measurements, suggests a relatively “clean” steel surface in the protected cells. Any layers, formed prior to CP application (as mentioned CP was applied at 120 days) would only bear conversions, but further oxidation of the steel will not occur in the time of protection. In the time of interrupting the CP however, and after depolarization for 24 h, allowing establishment of a steady OCP, the steel gradually slips to a more “active” state (as result of shifting the steel potential from strongly cathodic to natural for the present conditions potential). Taking into consideration the cement chemistry around the re-bars (chloride concentration above the thresholds of 0.15 w.% per dry cement weight (x)), in the period of electrochemical measurements, there will be conditions for steel dissolution on isolated locations, hence the recorded averaged corrosion current density might end up higher (lower  $R_p$  values respectively), comparing to corroding and non-corroding conditions.

As a second hypothesis, the nature of the product layer, formed on the steel surface (for each technical condition), is contributing to the performance of the systems and influencing the electrochemical response. Based on fundamentals, the measured corrosion current density will be controlled by the kinetics of the electrochemical reactions during the measurement and the diffusion of reactants both towards and away from the electrode. Hence, higher diffusion limitations, as in the corroding specimens, will result in effectively higher  $R_p$  values.

The above consideration is supported by the PDP measurements (Fig.6 left): the most significant anodic control in the region of 100 mV after  $E_{corr}$  is observed for the non-corroding specimen, followed by the corroding specimen. The impeded anodic reaction in the non-corroding specimen R is expected, as the steel surface is passive and the product layer is homogeneous. Comparing corroding specimen (3) and protected specimens (6 and 7) in the 100 mV region around  $E_{corr}$  in anodic direction, specimen 3 exhibits the highest limitations of the anodic reaction as result of heterogeneous and rough product layer on the steel surface. Basically, after the corrosion potential  $E_{corr}$ , an accelerated metal dissolution takes place at first. Considering that specimens 6 and 7 were protected before the time of the measurements, and the surface was initially preserved (less corrosion products than specimen 3), steel dissolution after  $E_{corr}$  is faster and formation of corrosion products takes place. Following the formation of these new layers, the dissolution is impeded due to diffusion limitations i.e. difficulties in the transport of pore solution to fresh metal surface on one hand and slower transport of soluble corrosion products back into the pore solution on the other. With anodic polarization further on (Fig.6 (left)) a trend towards continuous increase of current density is recorded. Further, approaching the region of maximal diffusion current and diffusion control (at relatively higher current densities) a steady state of the described process would take place. As conclusion, the higher  $R_p$  values for corroding specimen 3 are obviously attributed to diffusion limitations in conditions of external polarization and the product layers composition, which will be further discussed.



## 2. Microstructural and morphological observation.

Cross sections of the steel/cement paste interface were prepared for each technical condition. Visualization of the interface was obtained using ESEM in BSE mode (steel appears bright in the images), at different magnification up to 4000x. The investigation gives information for the adherence, thickness and distribution of the product layers on the steel surface.

Fig. 7 presents micrographs of the steel/cement paste interface for non-corroding (R), corroding (3), CP protected (6) and pulse CP protected (7) specimens at equal magnification (4000x). As seen from the micrographs, the most compact and adherent layer on the steel surface is the one in the non-corroding specimen R (Fig.7d). The product layers in the protected specimens exhibit similar compactness and adherence, the specimen 7 (pulse CP) however, characterized by a thinner and denser product layer ( $\sim 2\ \mu\text{m}$ ), compared to the product layer in specimen 6 (under conventional CP). In the former case the product layer is obviously more homogenous (Fig.7b), while in the latter case, the product layer is thicker ( $\sim 10\ \mu\text{m}$ ) and in addition presents a kind of multi-layered appearance (Fig.7a): a denser phase adhered to the steel (as in specimen 7) of about  $3\ \mu\text{m}$ , followed by a rough almost compact formation of  $\sim 4\ \mu\text{m}$  and a final non-compact, rough outer layer with low adhesion to the previous two of about  $2\ \mu\text{m}$  thickness. The product layer in the corroding specimen 3 (Fig.7c) exhibits the lowest adherence to the steel surface, very rough morphology, low density and lack of compactness i.e. exhibits the highest heterogeneity along with varying thickness of 3 to  $12\ \mu\text{m}$ .

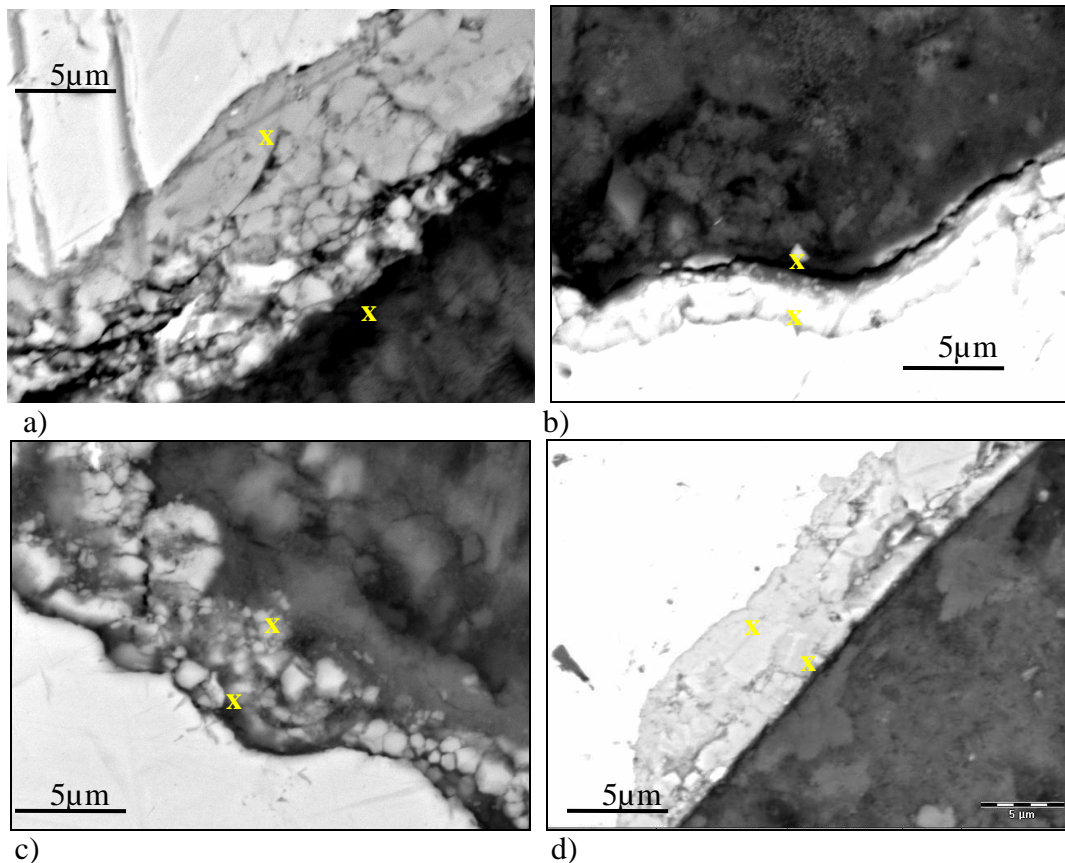


Fig. 7. Cross sections at magnification 4000x of the steel/cement paste interface in CP protected specimen 6 (a), pulse CP protected specimen 7 (b), corroding specimen 3 (c) and non-corroding specimen R (d)



The different appearance and properties of the product layers is obviously influencing the electrochemical response of the systems and is responsible for the systems behavior, when performing electrochemical measurements. It is known that the product layers on steel surface in  $\text{Ca}(\text{OH})_2$  environment (as in concrete or CE) are composed of several layers and in the simplest case are being considered as inner and strongly adherent formation, with composition similar to  $\text{Fe}_3\text{O}_4$  and a gelatinous outer layer of iron hydroxides, where  $\text{Fe}^{2+}/\text{Fe}^{3+}$  can be detected (32-34). Calcium ions can be incorporated in the outer atom layers of the inner layer and increase the protective ability of the product layers when no chlorides are present (34). Such case is relevant to the non-corroding specimen R. In the presence of chlorides, as in corroding specimens 3 and protected specimens 6 and 7 (both CP regimes were applied at 120 days after conditioning in SSC), the film thickness increases but the protective abilities decrease. Obviously with this respect, the pulse CP is more effective, compared to conventional CP, as specimen 7 exhibits more compact, thinner and adherent layer compared to specimen 6 (Fig.11 a,b), which proves the beneficial effects of the pulse current in terms of chloride withdrawn from the steel surface. This consideration is supported wet chemical analysis of the adherent cement paste as well – Fig.8.

The alkali concentrations around the steel bar are higher and the chloride concentration lower in the pulse CP conditions, compared to conventional CP. Here again, the observation supports the hypothesis for the beneficial effects of the pulse CP current, compared to conventional CP technique.

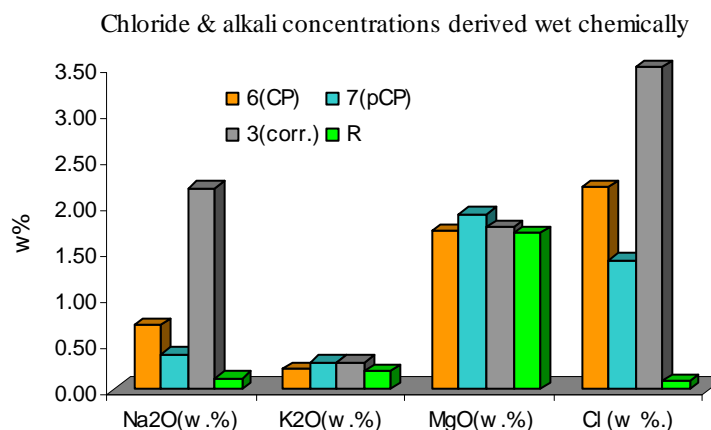


Fig. 8 Chloride and alkali concentration in the cement paste adjacent to the steel surface in w.% per dry cement weight, determined wet chemically (ASTM C1218).

The above statements suggest that the cement chemistry, as well as the composition of the product layers, have significant influence on the electrochemical parameters derived by EIS, PDP and RP measurements. Detailed information for the product layers composition, obtained by XRD and XPS, as well as surface layers morphology using longitudinal sections of steel surface from each technical condition is discussed in Part II of this work (35). Relevant to relationship of product layers parameters and composition with derived electrochemical parameters, the following could be considered:

There are several aspects that one should take into account when evaluating electrochemical performance of systems as in the present study in terms of product layers formation: One aspect is the substitution of iron oxides/hydroxides layers with calcium. This would cause structural changes in the oxide/hydroxide layers and will probably lead to different catalytic activity (4), hence will give difference in electrochemical parameters

obtained in different media (as concrete, CE and NaCl in the present study). Second aspect is the thickness, morphology and adhesion of the product layers. The protected specimen 7 for example, exhibits a thinner layer, composed of most likely  $\text{Fe}_3\text{O}_4$ , while specimen 6 exhibits a multi-layered formation, the outer layer being similar to the one in the corroding specimen 3. The outer layer of the corroding specimen 3 is most likely composed of non-adherent compounds as akaganeite and predominance of goethite and lepidocrocite, while for specimens 6,7 and R magnetite/hematite are the predominant products. These observations are consistent with reported results from similar research (36), where the presence of  $\alpha$ - and  $\gamma$ - $\text{FeOOH}$  are detected in the outer product layers, and  $\text{Fe}_3\text{O}_4$  and  $\alpha$ - $\text{FeOOH}$  in the inner layers. In addition to this sequence,  $\beta$ - $\text{FeOOH} \cdot \text{Cl}_2$  (akaganeite), being a needle shape formation at earlier age or bundles of rods of hollow subcrystals at later ages, is non-adherent compound, which does not accommodate in the product layer. Hence, the derived  $R_p$  values for the corroding specimen in concrete are higher than the protected cells, due to already discussed diffusion limitations, in addition to the larger surface area of the products, composing the surface layer in specimen 3 (as reported in (37) the surface area in  $\text{m}^2/\text{g}$  decreases in the sequence of:  $\text{Fe}_x\text{OH}_y \cdot z\text{H}_2\text{O} > \beta\text{-FeOOH} \cdot \text{Cl}_2 > \alpha\text{-FeOOH} > \alpha\text{-Fe}_2\text{O}_3$ ).

Along with the above considerations, another aspect is the conductivity (electron, ionic, electrical) of the formed layers. For example, electrical conductivity of goethite, hematite and magnetite is decreasing in the order: magnetite-hematite-goethite (38), which suggests that the layers containing mostly magnetite (as in specimens under pulse CP) will exhibit lower limitations to current flow (as in the time of electrochemical measurements), while specimens with high amounts of goethite (oxy-hydroxides are in higher amounts in the corroding specimens as consequence of more oxygen supply via micro-cracks) will exhibit higher resistivity to current flow.

Finally, if we consider some aspects of the passivity theory, an explanation for the highest  $R_p$  for the non-corroding specimens in all investigated mediums is the following: according to the film theory for example, the surface will be covered by oxygen containing thin layer, being a diffusion barrier. This film is formed predominantly on active points and defects on the surface. The film is with low ionic but good electron conductivity. In most cases this film is isolated by additional layer of non-stoichiometric oxides. The absorption theory suggests covering the surface by a mono-layer of absorbed oxygen, which limits the anodic dissolution process. The layer is initially not homogeneous and non-compact, covers at first only active points and defects. The passivity here is a result of chemisorption and the properties of the layer are different from the properties of the oxide phases. Both theories suggest a non-uniform but protective and high resistant layer on the steel surface, which if no aggressive substances are present (as in the non-corroding specimen R) might be further covered by additional phases relevant to the adjacent environment.

Apparently the product layers' physical and electrical properties, composition, crystallinity, adherence etc. are of significant importance for the interpretation of the electrochemical measurements on steel specimens in concrete (or in model medium). More detailed investigation of the above said features of the product layers on steel surface in corroding, non-corroding and cathodically protected conditions in correlation with electrochemical parameters is presently being performed and will be further reported by the present authors.

## Conclusions

The present study reveals the applicability of electrochemical measurements, namely EIS, PDP and PR for reinforced concrete not only with regard to corroding and non-corroding conditions but in case of cathodic protection as well.

Along with deriving polarization resistance values for the steel surface, EIS in concrete is a useful technique for accurately describing the electrical properties of the bulk matrix and gives information for the product layers formed on the steel surface in the different technical conditions, data readily applicable to modeling approaches in terms of mechanical behavior of such systems.

Further, microstructural analysis of the product layers, combined with morphological observations and chemical composition, suggest the basis of cathodic protection to be a compact, homogeneous and dense layer of mainly  $\text{Fe}_3\text{O}_4$ , strongly adhered to the steel surface.

The combination of methods reveals the fundamentals for cathodic protection effectiveness, which is normally evaluated according to empirical criteria only and additionally proves the efficiency of the introduced cost effective pulse CP as alternative of the conventional techniques.

## References

1. G.Glass et al., *Corr.Sci.*, 39 , 5, 1001-1013(1997)
2. V. Feliu, *JES* 151, B134 (2004)
3. K.Videm, *El.Acta* 46, 3895-3903 (2001)
4. C. Andrade et al., *El.Acta* 46, 3905 – 3912 (2001)
5. A.A.Sagues et al., *Corr.Sci* 45, 7-32 92003)
6. K.S.Kumar, *Corrosion*, 96, (1998)
7. Y. Choi et al., *Cor.Sci*, In press
8. M.F. Montemor et al., *Corr.Sci.*, 35 1571-1578 (1993)
9. S. Feliu et al., *Corr.Sci.*, 35, 1351-1358 (1991)
10. R. Cigna et al., *Corr.Sci.*, 35, 1579-1584, (1993)
11. K. Videm, *MatStrForum* 289-292 (1998), p3-14
12. J. Flis et al., *Corrosion* 49, No7 (1993)
13. V. Feliu et al., *Corrosion* 58, p.72, v.1 (2002)
14. J.M.R.Dotto et al., *Cem.Concr.Comp.*, 26, 31-39, (2004)
15. M.F.Montemor et al., *Cem.Concr. Comp.*, 24, 1, 45-53, (2002 )
16. V. Feliu et al., *Corr.Sci.*, 40, No.6, 975-993 (1998)
17. J.A.Gonzalez et al., *Corr.Sci.* 25, No.10, p.917-930 (1985)
18. J.A.Gonzalez *Corr.Sci.*, 25, No.7, p519 – 530 (1985)
19. G.Glass et al., *Corr.Sci.*, 37, 10, 1643-1646 (1995)
20. G.Glass et al., *Corr.Sci.*, 35 , 5-8, 1585-1592 (1993)
21. J.A.Gonzalez, *Corrosion* 61, v.1, (2005)
22. K. Ishii, H. Seki, T. Fukute, K. Ikwa, *Constr. &Build.Mater.*, 12, pp125-132 (1998)
23. J.J. Chang, *Cement Concrete Research* 32, pp 657-663 (2002)
24. D.A.Koleva, J.Hu, K.van Breugel, JHW de Wit, N.Boshkov, ECS Transactions, v.1 (ECS Los Angeles fall meeting 2005)
25. A.A. Sagues, S.C. Kranc, E.I. Moreno, *Corrosion Science* 37 (1995) 1097-1113.

26. MacDonald J.R., ed. , Impedance Spectroscopy, Emphasizing Solid materials and Systems, Wiley, NY (1987)
27. C. Andrade et al., *Cor.Sci.*, 37,v.12, pp2013-2023
28. Poupard et al., *CemConcrRes* 34, 6, 991-1000 (2004)
29. Wenger et al., *El.Acta*, 35, 10, 1573-1578 (1990)
30. Fedrizzi et al., *Cem.Concr.Res.*, 35, 3, 551-561 (2005)
31. D.A.Koleva, K.van Breugel, J.H.W.de Wit, J.Hu, “Advances in CP”, UMIST, Manchester, UK, [www.jcse.org](http://www.jcse.org)
32. O.A.Albani, J.O.Zerbino, J.R.Vilche, A.J.Arvia, *El.Acta*, v.31, 11, pp 1403-1411 (1986)
33. D.S.Leek, A.B.Poole in: Page C.L, Treadway K.W, Bamforth P.B., eds: Proceedings of the 3<sup>rd</sup> Intern.Symp.on Corrosion of Reinforcement in Concrete, London: Elsevier Appl. Sci. (1990), 67
34. H.Oranowska, Z.Szklarska-Smialowska, *Corr.Sci.*, v.21, 11, pp 735-747, (1981)
35. D.A.Koleva, J.H.W.de Wit, K.van Breugel, A.Fraaij, N.Boshkov, ECS v.2, *Denver meeting, manuscript No: F1-0328*
36. K.E.Garcia et al., *Hyperfine Interactions*, DOI 10.1007/s1075-005-9157-3 (2005)
37. S.E.O'Reilly, M.F. Hochella, *Geochim.&Cosmochim.Acta*, v.67, 23, pp4471-4487 (2003)
38. N. Guskos et al., *Mater.Research Bulletin*, 37, pp 1051-1061 (2002)